# Effect of Chain Lengths of *n*-Alcohol on the Formation of Single-Phase Microemulsions in *n*-Heptane/*n*-Alcohol/Sodium Dodecyl Sulfate/Water Systems

Isamu MIYATA,* Hiroshi MIYAMOTO, and Masakatsu YONESE

*Faculty of Pharmaceutical Sciences, Nagoya City University, Tanabe-dori, Mizuho-ku, Nagoya, 467, Japan.*
Received October 16, 1995; accepted December 27, 1995

**To elucidate the effects of chain lengths of alcohols (1-butanol, 1-hexanol, and 1-octanol) as cosurfactants on the formation of a single-phase microemulsion (L-region) in *n*-heptane/*n*-alcohol/sodium dodecyl sulfate (SDS)/water systems, the phase diagrams of pseudoternary systems were determined under a fixed SDS/alcohol weight ratio (=0.5). Conductivity, viscosity and light scattering intensity of the L-region were measured at 30 °C, and the results discussed from the microstructure of these systems. Using the SDS-free model system, the distribution of alcohol and the interfacial tension between oil (heptane) and water phases were measured in the presence of alcohol. The difference in distribution of alcohols resulting from differences in the chain lengths was found to be one of the key factors determining the extensions of the region of microemulsion and the microstructures. The L-regions in the hexanol and octanol systems were much smaller than in the butanol system. The continuous phases of these systems were the oil-rich medium (water-in-oil-type) throughout the L-region with increasing the water content. The L-region in the butanol system, on the other hand, was larger and the continuous phases of this system changed gradually from the oil-rich to the water-rich medium (oil-in-water-type) through the bicontinuous medium (bicontinuous-type) with increasing the water content.**

**Key words** microemulsion; cosurfactant; phase diagram; electric conductivity; viscosity

Microemulsions are transparent, homogeneous systems which generally consist of water, oil, surfactant and cosurfactant. They are thermodynamically stable and spontaneously formed. Microemulsions are generally prepared by adding medium chain length alcohols as cosurfactant to an emulsion system which is thermodynamically unstable. Microemulsions have been studied fundamentally by Schulman *et al.*[1-4] and Winsor,[5] and recently the studies have made extensive progress using electric conductivity,[6-11] viscosity,[12-14] light scattering,[15-18] fluorescence[19-21] and so on. Microemulsions are classified into three types of continuous phases: The first is an oil-in-water (O/W)-type microemulsion in which an oil droplet is dispersed into the water phase. The second is a water-in-oil (W/O)-type microemulsion in which a water droplet is dispersed into the oil phase. The third is a bicontinuous-type microemulsion[22] in which oil and water phases are randomly intermixed.

Microemulsions are very useful in industrial fields, particularly for oil recovery and can be also applied as micro-reactors by utilizing the characteristics of the microenvironment such as the water structure they contain. In the field of pharmaceutical sciences, microemulsions have recently attracted special interest as vessels of drug delivery systems (DDS). However, there have been only a few studies on their applicability.[23-28] Determination of the phase diagrams and the microstructure of a microemulsion is significant in elucidating the role of cosurfactants. In this study *n*-heptane as an oil, sodium dodecyl sulfate (SDS) as a surfactant and *n*-alcohols (1-butanol, 1-hexanol, and 1-octanol) as cosurfactants were used. The phase boundaries of the transparent single-phase region of each alcohol system were precisely determined and the phase diagrams in pseudoternary systems were obtained under a fixed SDS/alcohol weight ratio at constant temperature. The effect of the chain length of alcohol on the formation of the single-phase microemulsion was determined by measuring conductivity, viscosity and light scattering intensity in the single-phase region of each alcohol system. The distribution of alcohol and the interfacial tension between heptane and water phases were measured using SDS-free model systems (ternary *n*-heptane/*n*-alcohol/water systems) to estimate the role of alcohol.

## Experimental

**Materials** *n*-Heptane was obtained from Katayama Chemical Ind. Co., Ltd. (special grade, assay: 99%). 1-Butanol, 1-hexanol, and 1-octanol were obtained from Katayama Chemical Ind. Co., Ltd. (special grade for all alcohols, assay: 99%, 99%, and 98%, respectively). SDS was obtained from Wako Pure Chemical Ind., Ltd. (biochemical use grade). From the molar electric conductivity *vs.* the square root of the concentration relationship, the value of critical micelle concentration (cmc) for obtained SDS was determined to be 8.0 mmol·dm$^{-3}$ in aqueous solution at 25 °C. All these materials were used without any further purification except for distribution of alcohol and interfacial tension measurements. For these two measurements, *n*-heptane and *n*-alcohol were distilled twice. Deionized and distilled water was used, and its electrolytic (specific) conductivity was lower than $0.3 \times 10^{-6}$ S cm$^{-1}$ at room temperature. Methyl orange and sudan III used as dyes were obtained from Katayama Chemical Ind. Co., Ltd. (special grade) and Wako Pure Chemical Ind., Ltd. (special grade), respectively, and used without any further purification.

**Methods** The optimal value of the SDS/alcohol weight ratio, $R$, was chosen from a group to be 0.5 in this experiment, *i.e.*, $\alpha$-plane (pseudo-ternary phase diagram) of the tetrahedron diagram shown in Fig. 1, since a single-chain surfactant such as SDS would not form a microemulsion until $R$ is lower than 0.5, based on geometric considerations.[22,29,30]

The phase diagrams were determined by preparing the samples with various compositions on $\alpha$-plane. The samples were thoroughly shaken and then allowed to equilibrate in a thermostated bath for at least 15 d at 30 °C. Then, the phase boundaries of the transparent single-phase region of each alcohol system were precisely determined by the water titration method.[31]

Conductivity, viscosity and light scattering intensity were measured in the transparent single-phase region on $\alpha$-plane of the tetrahedron

* To whom correspondence should be addressed.

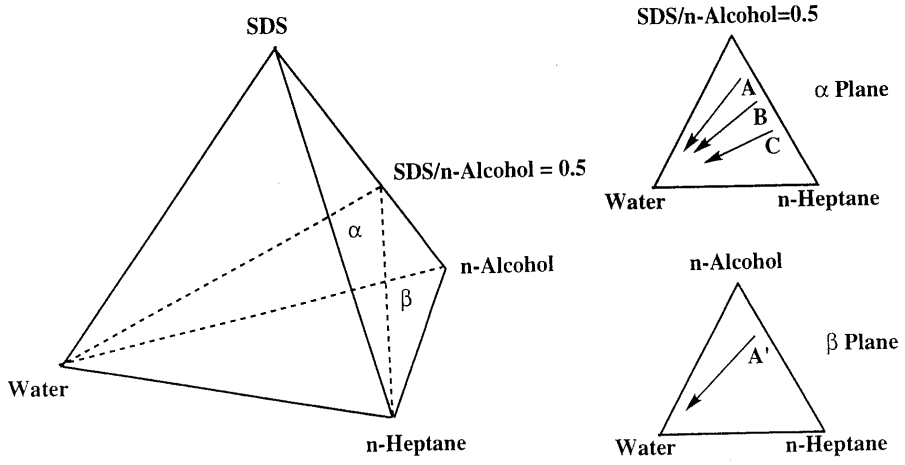


Fig. 1. Schematic Tetrahedron Diagram of *n*-Heptane/*n*-Alcohol/SDS/Water System

α-Plane (SDS/alcohol=0.5): A line, (SDS+alcohol)/heptane=4.0; B line, (SDS+alcohol)/heptane=1.5; C line, (SDS+alcohol)/heptane=0.67. β-Plane (SDS-free): A′ line, projection of A line from SDS apex.

diagram shown in Fig. 1. Conductivities were measured by a CM-40S Conductmeter (Toa Electronics, Ltd.) along each line (A, B and C lines being the weight ratio of (SDS+alcohol)/heptane=4.0, 1.5, 0.67, respectively) on α-plane. With addition of water to a sample solution of a fixed composition of SDS, alcohol and heptane, conductivities were successively measured under constant stirring at 30 °C, and their values were recorded after they became constant. Viscosity and light scattering intensity were measured by an ELD viscometer of cone-plate type (Tokimec Co., Ltd.) and a DLS 700-Ar (Otsuka Electric Co., Ltd.) along the A line on α-plane at 30 °C.

The distribution of alcohol and the interfacial tension between the oil (heptane) and water phases were measured along A′ line in the two liquid-phase region on β-plane (ternary phase diagram with SDS-free, $R=0$) of the tetrahedron diagram shown in Fig. 1. The mixed solutions composed of heptane, alcohol and water were shaken in a thermostatic bath at 30 °C for at least 1 d. After reaching the equilibrium of the distribution, the concentrations of alcohol in the heptane phase were determined by a GC-3BT gas chromatography (Shimadzu Co., Ltd.), of which the column packing agent (Wako Pure Chemical Ind., Ltd.) was polyethylene glycol 20M and Chromosorb W (solid support). Concentrations in the water phase were obtained by subtracting from the total amounts of alcohol.

The interfacial tensions between the heptane and water phases in the presence of alcohols were measured by a Du Noüy surface and interfacial tensionmeter (Shimadzu Co., Ltd.) along A′ line on β-plane at 30 °C. The samples for the interfacial tension measurement were prepared in the same manner as the distribution measurement.

## Results and Discussion

**Phase Diagrams** Figure 2 shows the phase diagrams of 1-butanol, 1-hexanol, and 1-octanol systems on α-plane at 30 °C. The L-region in the phase diagrams denotes the transparent single-phase. From these results, the L-region in the butanol system was found to be much larger than that in the hexanol and octanol systems extending nearly to the water apex, while in the latter two systems it extended only up to 40—45% water content at most. The difference in extensions of the L-region in these phase diagrams depended on the solubility of the alcohols in water. Actually, butanol is quite soluble in water, while hexanol and octanol is almost insoluble. The significance of the solubility of alcohol in water was also shown from the phase diagram in the propanol (well soluble in water) system[32] which was very similar to that in butanol system.

Determination of the continuous phase of the L-region was attempted with the dye method, using methyl orange as a water-soluble dye and sudan III as an oil-soluble dye. Dropping the dye solution (0.1% methyl orange in water and 0.1% sudan III in heptane) into the sample solutions in the L-region, the dissolution process and the states of the droplets of the dye solutions were observed. In the hexanol and octanol systems, the droplet of methyl orange solution precipitated in the sample solutions throughout the whole L-region and that of sudan III solution diffused into them. The continuous phases in the hexanol and octanol systems are thus the oil-rich medium throughout the L-region. In the butanol system, in contrast, the dissolution states of the dyes varied with the water content, $W_w$, in the L-region. In the case of $W_w > 60\%$, the droplet of methyl orange solution diffused into the sample solutions and that of sudan III solution floated on the surface. In the case of $60\% > W_w > 10\%$, both methyl orange and sudan III solution droplets diffused slowly into the sample solutions. With decreasing $W_w$, as when $W_w < 10$—15%, the droplet of methyl orange precipitated and sudan III solution diffused into the sample solutions. From these results, the continuous phase in the butanol system was suggested to vary gradually from the oil-rich to the water-rich medium, through the bicontinuous medium with increasing $W_w$.

**Distributions of Alcohol and Interfacial Tensions between Oil and Water Phases** The distribution of alcohol and the interfacial tension between oil (heptane) and water phases affected the extensions of the L-region in the phase diagram. In the SDS added system, however, the values of the interfacial tension were so low and the interface was so disturbed even with the addition of 1 mmol $kg^{-1}$ SDS to the water that it was difficult to measure the interfacial tension using the ordinary Du Noüy ring method. Therefore, *n*-heptane/*n*-alcohol/water systems were used as a basic model in an SDS-free condition, and the interfacial tension and the distribution of alcohol between heptane and water phase were measured to estimate the effect of chain lengths of alcohol on the formation of the single-phase microemulsion.

The distribution ratios of alcohol between heptane and water phases in SDS-free systems were determined along

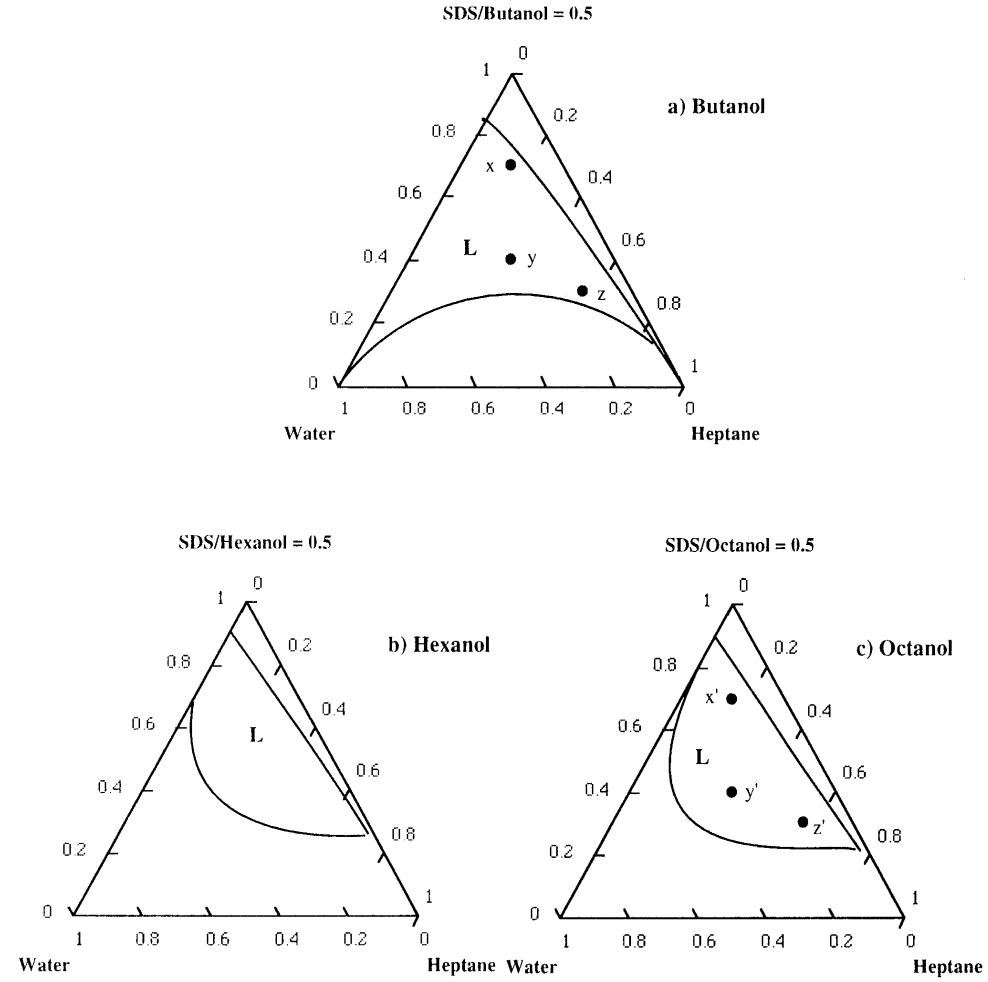


Fig. 2. Partial Pseudoternary Phase Diagrams for *n*-Heptane/*n*-Alcohol/SDS/Water Systems at 30 °C

L: transparent single-phase region. a) Butanol system: x: 15% heptane, 15% water, 70% (SDS + butanol); y: 30% heptane, 30% water, 40% (SDS + butanol); z: 56% heptane, 14% water, 30% (SDS + butanol). b) Hexanol system. c) Octanol system: x′: 15% heptane, 15% water, 70% (SDS + octanol); y′: 30% heptane, 30% water, 40% (SDS + octanol); z′: 56% heptane, 14% water, 30% (SDS + octanol).

A′ line on $\beta$-plane in the tetrahedron diagram of Fig. 1. A′ line is the projection of A line on $\alpha$-plane, and the composition of A′ line corresponds to that of A line except it is SDS-free. The distribution ratios, $P$, of butanol between heptane and water phases are shown in Fig. 3 as a function of the water content, $W_w$. $P$ was defined as

$$P = C_a^h / C_a^w , \quad (1)$$

where $C_a^h$ and $C_a^w$ are molar concentrations of alcohol in heptane and water phases, respectively. For octanol system, the values of $P$ were infinity, and thus octanol was confirmed to be distributed only in the heptane phase. Butanol, on the other hand, was distributed not only in the heptane phase but also in the water phase and the values of $P$ were in the range 7.4—8.0. The difference in $P$ between butanol and octanol would affect significantly the interfacial tension between heptane and water phases.

The interfacial tensions, $\sigma$, between heptane and water phases in the presence of butanol or octanol are shown in Fig. 4 as a function of the water content, $W_w$, along A′ line on $\beta$-plane; the interfacial tension without alcohol was *ca.* 52 mN m$^{-1}$. Addition of alcohol to the heptane–water two phase system significantly reduced the interfacial tensions between heptane and water phases, as pointed out by Overbeek.[33] In the butanol system the interfacial tensions are very low at *ca.* 1 mN m$^{-1}$, but in the octanol system these interfacial tensions are relatively high at *ca.* 8 mN m$^{-1}$.

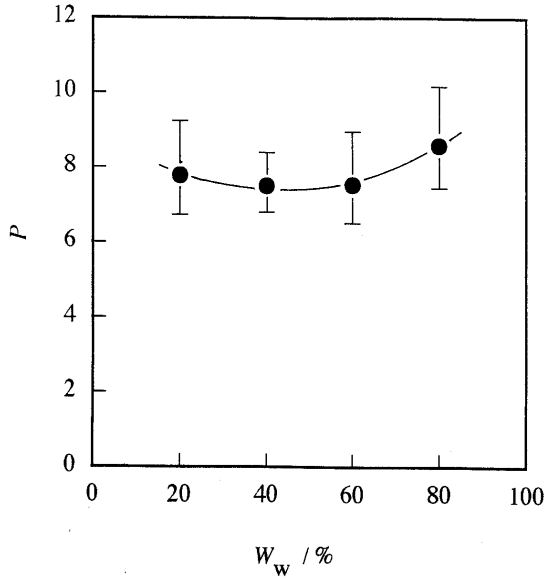


Fig. 3. Distribution Ratio of Butanol, $P$, *vs.* Water Content, $W_w$, for *n*-Heptane/1-Butanol/Water Systems along A′ Line in $\beta$-Plane at 30 °C

The interfacial tensions of an *n*-heptane/*n*-alcohol/water

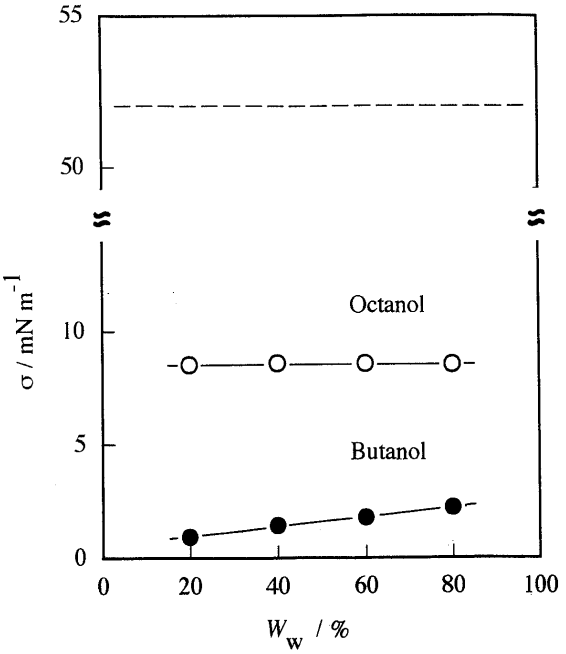


Fig. 4. Interfacial Tension, $\sigma$, *vs.* Water Content, $W_w$, for *n*-Heptane/*n*-Alcohol/Water Systems along A′ Line in $\beta$-Plane at 30 °C

●, butanol system; ○, octanol system; ------, alcohol-free.

system would decrease significantly with the addition of SDS. In the butanol system, they are expected to reach zero much more easily than in the octanol system, as estimated from the results of Zhou and Dupeyrat.[34] They measured the interfacial tensions between dodecane and water phases in the presence of butanol and SDS using a spinning drop tensionmeter at 25 °C, and reported that the minimum interfacial tension in a system containing 13.8% butanol is *ca.* 0.2 mN m$^{-1}$ at above 8 mmol dm$^{-3}$ SDS in water. Thus, the addition of butanol into a heptane/SDS/water system causes the interfacial tension to decrease significantly, that is, the interfacial area more easily increases, so that the continuous phase of the L-region in the butanol system can change from the oil-rich to the water-rich medium, through the bicontinuous medium with increasing $W_w$. The relatively high interfacial tension in the octanol system makes it more difficult to reach zero, so that the continuous phase of the L-region in this system cannot change from oil-rich, and the resultant water droplet becomes larger with increasing $W_w$. Characteristics of the single-phase microemulsion region of each alcohol system were then investigated in detail.

**Characteristics of Single-Phase Microemulsion Regions**

Conductivity: Electrolytic conductivities, $\kappa$, of butanol,

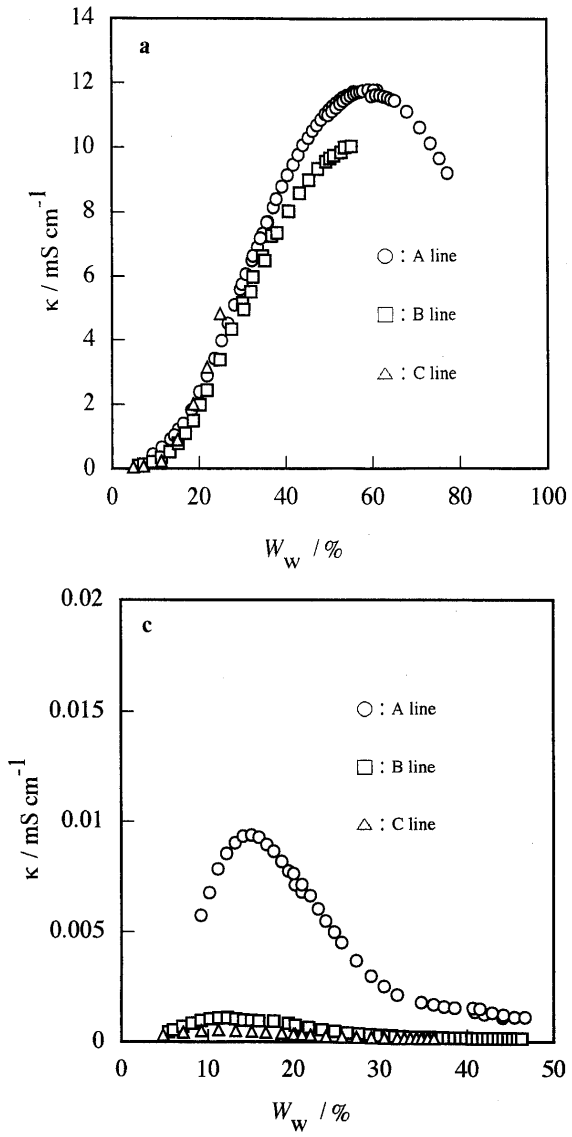


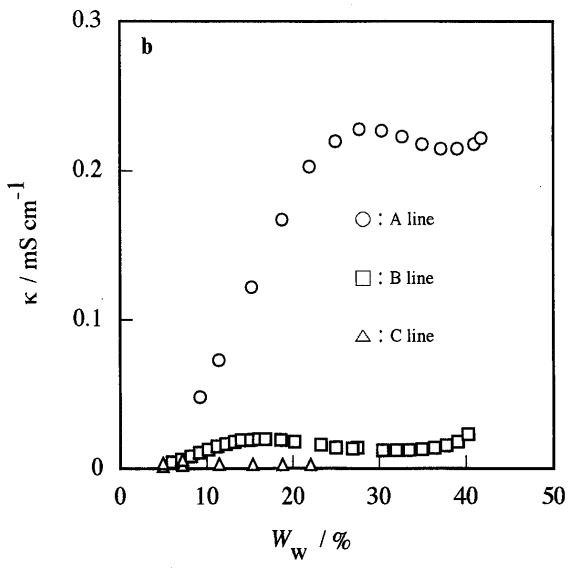


Fig. 5. Electrolytic Conductivity, $\kappa$, *vs.* Water Content, $W_w$, for *n*-Heptane/*n*-Alcohol/SDS/Water Systems along Each Line in $\alpha$-Plane at 30 °C

a) Butanol system; b) hexanol system; c) octanol system. ○, A line; □, B line; △, C line.

hexanol and octanol systems are shown in Fig. 5a, b and c as a function of the water content, $W_w$, along A, B and C lines on $\alpha$-plane. As shown in Fig. 5a, the values of $\kappa$ in the butanol system rapidly increased from the magnitude of $\mu S \cdot cm^{-1}$ to $mS \cdot cm^{-1}$ with increasing $W_w$ as expected from the so-called percolation behavior of microemulsion,[7-10] which indicates that the conducting paths are being formed. The values of $\kappa$ in the hexanol and octanol systems did not greatly change and maintained the order of $\mu S \cdot cm^{-1}$ with increasing $W_w$ as shown in Fig. 5b and c, respectively. The microstructures of the L-region obtained with the dye method were confirmed further by these conductivity data. Namely, in butanol system, the continuous phases of the L-region gradually change from the oil-rich to the water-rich medium through the bicontinuous medium with increasing $W_w$, and thus the conductive path expands in the bulk phase. In the hexanol and octanol systems, on the other hand, since the conductivities are very low, the continuous phases of the L-region are the oil-rich medium throughout this region even with increasing $W_w$.

The maximum conductivity in the neighborhood of 60% water content as shown in Fig. 5a is believed to be the transition point from the bicontinuous to the water-rich medium in the L-region, and the decrease of conductivity with increasing $W_w$ results from the decrease of SDS molecules as the transmitter of electricity. The differences of plots of A, B and C lines in Fig. 5b and c are related to the SDS content.

Light Scattering Intensity: The light scattering intensities, $I$, of each alcohol system at the angle of 90 degrees and the wavelength of 488 nm (Ar laser) are shown in Fig. 6 as a function of the water content, $W_w$, along A line on $\alpha$-plane. In hexanol and octanol systems, the values of $I$ rapidly increased with increasing $W_w$ and the phase separations occurred. These results suggested that the water droplets in the hexanol and octanol systems become larger with increasing $W_w$ and decrease with the amount of SDS. In the butanol system the values of $I$ did not change as much as in the hexanol and octanol systems with increasing $W_w$, and the maximum was found at $W_w = 60$—70%. In the region of the bicontinuous medium ($15\% < W_w < 60\%$) along A line, the values of $I$ were found to increase slightly and in the region of the water-rich medium ($W_w > 60\%$) to decrease. The slight increase of $I$ is thought due to the successive change of the continuous phase of L-region.

The two patterns of light scattering intensity result from the difference in the continuous phases. The pattern observed for the butanol system indicates that the con-

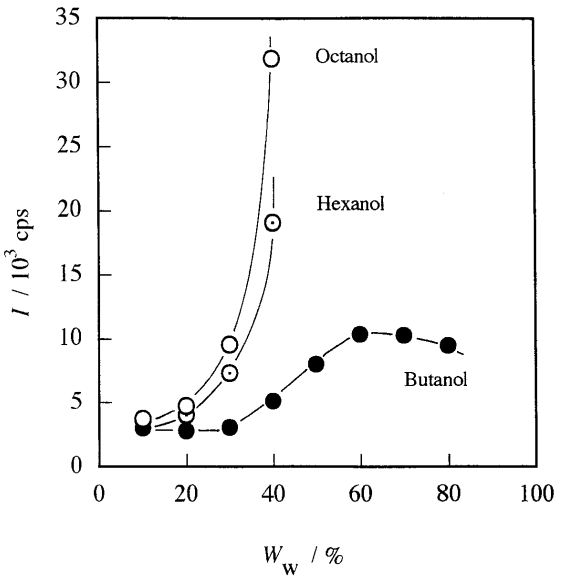


Fig. 6. Light Scattering Intensity, $I$, at the Angle of 90 Degrees and the Wavelength of 488 nm (Ar Laser) *vs.* Water Content, $W_w$, for *n*-Heptane/*n*-Alcohol/SDS/Water Systems Along A Line in $\alpha$-Plane at 30 °C

●, butanol system; ⊙, hexanol system; ○, octanol system.

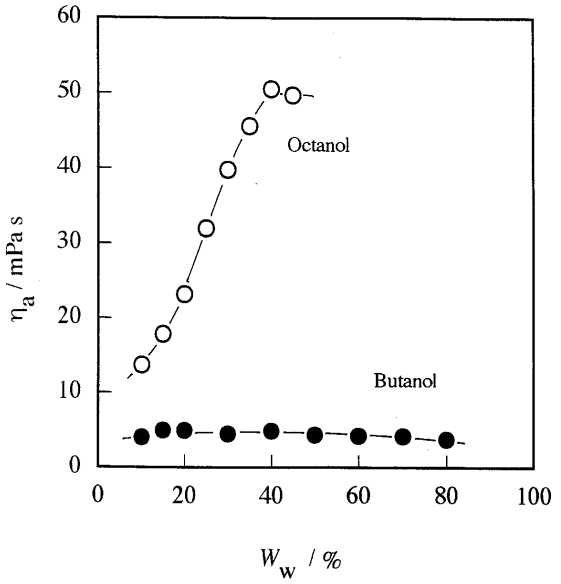


Fig. 7. Apparent Viscosity, $\eta_a$, at Shear Rate, $D_s = 38.3\,s^{-1}$, *vs.* Water Content, $W_w$, for *n*-Heptane/*n*-Alcohol/SDS/Water Systems along A Line in $\alpha$-Plane at 30 °C

●, butanol system; ○, octanol system.

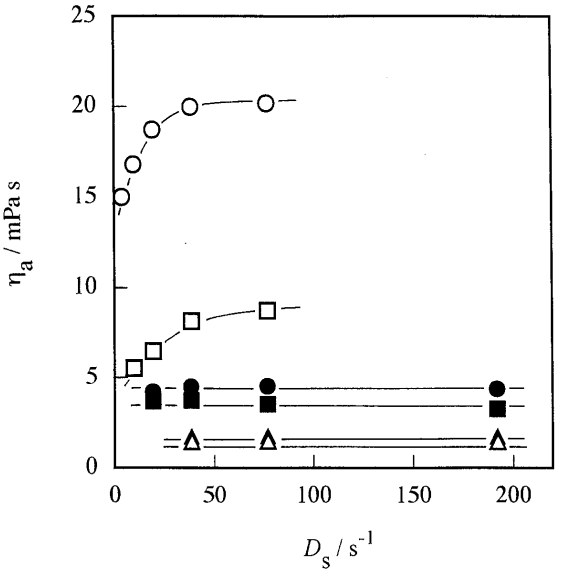


Fig. 8. Apparent Viscosity, $\eta_a$, *vs.* Shear Rate, $D_s$, at Each Composition Point (x, y, z, x′, y′ and z′) for *n*-Heptane/*n*-Alcohol/SDS/Water Systems at 30 °C

●, butanol system at x; ■, butanol system at y; ▲, butanol system at z; ○, octanol system at x′; □, octanol system at y′; ▲, octanol system at z′. Compositions of x, y, z, x′, y′ and z′ are shown in Fig. 2.

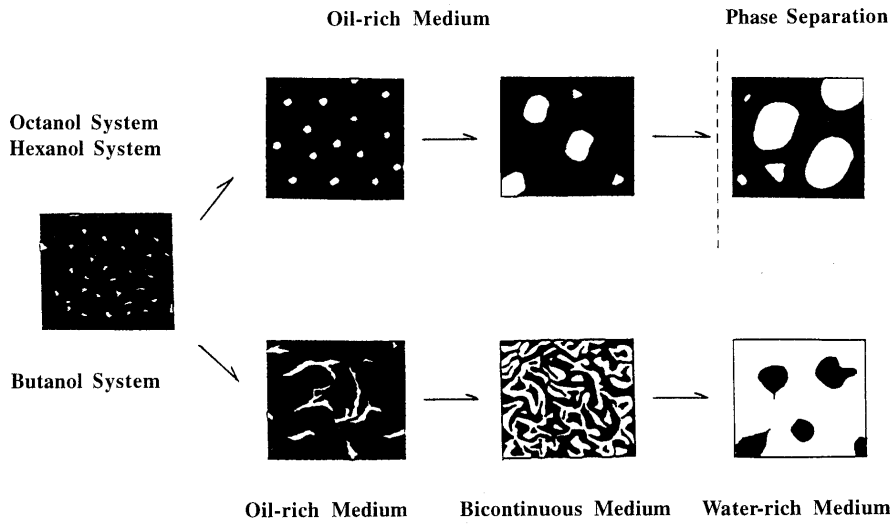


Fig. 9. Schematic Diagrams of Microstructural Changes in Single-Phase Microemulsion with Increasing Water Content
Dark part, oil-rich phase; white part, water-rich phase.

tinuous phase gradually changes from the oil-rich to the water-rich medium through the bicontinuous medium with increasing $W_w$. The other pattern observed for the hexanol and octanol systems indicates that the continuous phase maintains an oil-rich medium throughout the L-region. In the following section, the viscosities were measured focusing on the butanol and octanol systems.

Viscosity: The apparent viscosities, $\eta_a$, of butanol and octanol systems at shear rate, $D_s = 38.3\,s^{-1}$ are shown in Fig. 7 as a function of the water content, $W_w$, along A line on $\alpha$-plane. In the octanol system, the values of $\eta_a$ increased rapidly with increasing $W_w$. This increase results from the increase in size of the water droplets as expected from Einstein's viscosity equation. In the butanol system, the change of $\eta_a$ was not as significant, and in the region of the bicontinuous medium ($W_w = 15$—$60\%$) along A line, the values of $\eta_a$ were found to change only slightly. These results were believed due to the successive change in the continuous phase of the L-region as well as to the light scattering intensity. In the region of the bicontinuous medium, the reason for the slight change in viscosity should be examined further as well as the reason for the slight increase in the light scattering intensity shown in Fig. 6.

To elucidate the properties of fluids throughout the L-region, the viscosities of all samples in the region were measured at various shear rates, $D_s$. The samples used for each measurement were prepared so that the effect of the previous shear was removed. Examples of the viscosity changes are shown in Fig. 8 as a function of $D_s$. The compositions of the systems in Fig. 8 are denoted by ● marks in Fig. 2. The properties of the fluids in the L-region in the octanol system were dependent on the system compositions, *i.e.*, in the oil-rich region more than 50% heptane Newtonian flows were observed because the viscosities did not change with increasing $D_s$, while less than 50% heptane non-Newtonian flows were observed in this region. These non-Newtonian flows are thought to result from the increase in the size and number of the W/O-type microemulsion droplets as judged by the magnitude of the light scattering intensities and the viscosities. The properties of the fluids throughout the L-region in the butanol system were found to be Newtonian flows because of the low constant viscosities.

From characteristics of the single-phase microemulsion regions described above, the single-phase microemulsions in *n*-heptane/*n*-alcohol/SDS/water systems were found to have two patterns of microstructural changes depending on the chain length of alcohol, which affects the distribution of alcohol and the interfacial tension between oil and water phases. For the butanol system it changes successively from W/O-type to O/W-type through the bicontinuous-type with increasing $W_w$. While, for the hexanol and octanol systems it retains W/O-type throughout the L-region.

**Macroscopic View of Microstructural Changes in Single-Phase Microemulsion** Based on the characteristics of the single-phase microemulsion regions described above, the microstructures of these microemulsions in *n*-heptane/*n*-alcohol/SDS/water systems were found to depend on the chain length of alcohol. On the basis of the discussions in previous sections, Fig. 9 shows schematic diagrams of the microstructural changes in the single-phase microemulsion with increasing $W_w$ along A line on $\alpha$-plane. Our results are summarized as follows. In the octanol and hexanol systems the continuous phases were the oil-rich medium (W/O-type) throughout L-region even in high $W_w$, in which the water droplets become larger and finally the phase separation occurs. In the butanol system the continuous phase gradually changed from the oil-rich (W/O-type) to the water-rich medium (O/W-type) through the bicontinuous medium (bicontinuous-type) in which water and oil part are randomly mixed. The difference of the microstructural changes owing to the carbon number of alcohols is thought to result from the difference in the distribution of these alcohols and that of the interfacial tension between oil (heptane) and water phases.

**References**

1) Hoar T. P., Schulman J. H., *Nature* (London), **152**, 102—103 (1943).
2) Schulman J. H., McRoberts T. S., *Trans. Faraday Soc.*, **42B**, 165—170 (1946).

3) Schulman J. H., Riley D. P., *J. Colloid Sci.*, **3**, 383—405 (1948).
4) Schulman J. H., Stoeckenius W. S., Prince L. M., *J. Phys. Chem.*, **63**, 1677—1680 (1959).
5) *a*) Winsor P. A., *Trans. Faraday Soc.*, **44**, 376—382 (1948); *b*) *Idem*, *ibid.*, **46**, 762—772 (1950).
6) Mackay R A., Agarwal R., *J. Colloid Interface Sci.*, **65**, 225—231 (1978).
7) Lagourette B., Peyrelasse J., Boned C., Clausse M., *Nature* (London), **281**, 60—62 (1979).
8) Ninham B. W., Chen S. J., Evans D. F., *J. Phys. Chem.*, **88**, 5855—5857 (1984).
9) Fang J., Venable R. L., *J. Colloid Interface Sci.*, **116**, 269—277 (1987).
10) Bisal S., Bhattacharya P. K., Moulik S. P., *J. Phys. Chem.*, **94**, 350—355 (1990).
11) Ray S., Bisal S. R., Moulik S. P., *J. Chem. Soc., Faraday Trans.*, **89**, 3277—3282 (1993).
12) Rushforth O. S., Sanchez-Rubio M., Sabtos-Vidals L. M., Wormuth K. R., Kaler E. W., Cuevas R., Puig J. E., *J. Phys. Chem.*, **90**, 6668—6673 (1986).
13) Borkovec M., Eicke H.-F., Hammerich H., Gupta B. D., *J. Phys. Chem.*, **92**, 206—211 (1988).
14) Ayyub P., Maitra A., Shah D. O., *J. Chem. Soc., Faraday Trans.*, **89**, 3585—3589 (1993).
15) Hermansky C., Mackay R. A., *J. Colloid Interface Sci.*, **73**, 324—331 (1980).
16) Kaler E. W., Prager S., *J. Colloid Interface Sci.*, **86**, 359—369 (1982).
17) Siano D. B., Myer P., Bock J., *J. Colloid Interface Sci.*, **117**, 534—543 (1987).
18) Beckman E. J., Smith R. D., *J. Phys. Chem.*, **94**, 3729—3734 (1990).
19) *a*) Lianos P., Lang J., Strazielle C., Zana R., *J. Phys. Chem.*, **86**, 1019—1025 (1982); *b*) Lianos P., Lang J., Zana R., *ibid.*, **86**, 4809—4814 (1982); *c*) Lianos P., Lang J., Sturm J., Zana R., *ibid.*, **88**, 819—822 (1984).
20) Aoudia M., Rodgers M. A. J., Wade W. H., *J. Colloid Interface Sci.*, **144**, 353—362 (1991).
21) Zhang J., Fulton J. L., Smith R. D., *J. Phys. Chem.*, **97**, 12331—12338 (1993).
22) Evans D. F., Mitchell D. J., Ninham B. W., *J. Phys. Chem.*, **90**, 2817—2825 (1986).
23) Osborne D. W., Ward A. J. I., O'Neill K. J., *Drug Develop. Ind. Pharm.*, **14**, 1203—1219 (1988).
24) Fubini B., Gasco M. R., Gallarate M., *Int. J. Pharm.*, **50**, 213—217 (1989).
25) Osborne D. W., Ward A. J. I., O'Neill K. J., *J. Pharm. Pharmacol.*, **43**, 451—454 (1991).
26) Willimann H., Walde P., Luisi P. L., Gazzaniga A., Stroppolo F., *J. Pharm. Sci.*, **81**, 871—874 (1992).
27) Malcolmson C., Lawrence M. J., *J. Pharm. Pharmacol*, **45**, 141—143 (1993).
28) Thacharodi D., Rao K. P., *Int. J. Pharm.*, **111**, 235—240 (1994).
29) Oakenfull D., *J. Chem. Soc., Faraday Trans. 1*, **76**, 1875—1886 (1980).
30) Zemb T. N., Hyde S. T., Derian P.-J., Barnes I. S., Ninham B. W., *J. Phys. Chem.*, **91**, 3814—3820 (1987).
31) Lagues M., Sauterey C., *J. Phys. Chem.*, **84**, 3503—3508 (1980).
32) Miyata I., Sakura T., Yonese M., *J. Jpn. Oil Soc.*, "submitted."
33) Overbeek J. T. G., *Adv. Colloid Interface Sci.*, **15**, 251—277 (1982).
34) Zhou J. S., Dupeyrat M., *J. Colloid Interface Sci.*, **134**, 320—335 (1990).